Measurement of Z+ Jets Cross-Section at ATLAS

The ATLAS collaboration

Abstract

The production of a W or Z boson in conjunction with jets is an interesting process in its own right as well as a signal channel (and background) for many interesting standard model and beyond standard model physics processes. The wide kinematic range for production of W/Z + jets serves as a testing ground for perturbative QCD predictions, both fixed order alone, and in conjunction with parton shower Monte Carlos. Final states with 2,3,4 or more jets accompanying a W/Z boson will be relatively common at the LHC and will serve as an important part of the ATLAS physics program. In this note, we will concentrate on Z + jets final states.

The reconstruction of leptons and of missing transverse energy becomes more complex in the presence of a multi-jet final state. We will quantify, in this note, the reconstruction differences with respect to those observed in inclusive Z production. We will calculate the rates for Z plus up to five or more jets, and will compare predictions from next-to-leading order perturbative QCD calculations (where available) to those from leading order matrix element and parton shower Monte Carlo programs. The systematic and statistical errors expected in the first inverse femtobarn of data will be compared to the theoretical pdf uncertainties for the predicted cross sections.

1 Introduction

In this note, we consider the triggering, reconstruction and analysis of events containing a Z boson plus jets in ATLAS. Due to a shortage of space, results will be quoted only for Z + jets final states, but with techniques applicable to the case of W + jets as well. We concentrate on channels with decays into electrons and muons, ignoring for the moment taus (except to account for backgrounds to the other decay channels). Much of the effort on the triggering and reconstruction of leptons is in common with the inclusive W/Z note [1]; thus, we do not reproduce all of the details from that note, but rather comment on the impact of a multijet environment on these issues. Fully simulated signal and background event samples are treated as pseudo-data. Comparisons of the reconstructed/corrected quantities, when possible, are made to the generated Monte Carlo hadron information (and in some cases to parton-level information with parton-to-hadron corrections applied). Our primary end-results are hadron-level cross-sections, similar to what will be available with the real ATLAS data. We present expectations/yields/systematics scaled to $1\,\mathrm{fb}^{-1}$, an integrated luminosity that should be accumulated within the first two years of running. Errors due to a miscalibration of the jet energy scale (JES) are expected to be the dominant systematics for the determination of Z + jets cross-sections. We compare the impacts of JES uncertainties of 1, 3 and 10% on the precision of the Z + jets cross sections.

2 Reference Cross-Sections and Monte Carlo Datasets

Reference cross-sections are collected in [2], but we briefly discuss here the cross-sections relevant for this note. NLO is the first order at which the Z + jets cross-sections have a realistic normalization (and realistic shapes for some kinematic distributions) [3]. The current state of the art for NLO calculations is for Z + 2 jets, although there is ongoing work for the calculation of 3 jet final states. Cross-sections for Z + 0, 1 and 2 (3) jet final states can be conveniently calculated at LO and NLO (LO only) using the MCFM [4] program, and it is from this program that we determine our reference cross-sections. The MCFM cross-sections were generated using the CTEQ6.1 PDFs [5] and a renormalization/factorization scale of $m_Z^2 + p_{T,Z}^2$, with similar kinematic cuts on the leptons and jets as will be described in Section 3.

2.1 Monte Carlo Datasets

Most of the Monte Carlo samples used in these studies are generated with ALPGEN [6] interfaced with HERWIG [7] using the leading order PDF set CTEQ6LL [8]. The cross-sections are calculated using a renormalization/factorization scale of $m_Z^2 + p_{T,Z}^2$, equal to that used for the MCFM predictions. The full datasets are obtained by merging samples of $Z + 0$ up to 5 partons, weighted according to the expected cross-sections, with an MLM [6] matching cut at $p_T > 20$ GeV [1], and normalized to an integrated luminosity of $1\,\mathrm{fb}^{-1}$. All datasets correspond to exclusive samples, with the exception of the highest multiplicity sample ($Z + 5$ partons) which is inclusive. The samples correspond to the decays, $Z \rightarrow e^+e^-$ and $Z \rightarrow \mu^+\mu^-$. A generator-level filter requires one Monte Carlo jet of $p_T > 20$ GeV and $|\eta| < 5.0$ and two electrons/muons with $p_T > 10$ GeV and $|\eta| < 2.7$ in the event. PYTHIA [10] signal and background samples are also produced, using the standard ATLAS underlying event tune. PYTHIA $Z \rightarrow e^+e^-(Z \rightarrow \mu^+\mu^-)$, events are generated with a generator-level filter requiring one Monte Carlo electron (muon) with $p_T > 10(p_T > 5)$ GeV and $|\eta| < 2.7(< 2.8)$. PYTHIA $Z \rightarrow \tau^+\tau^-$

---

[1] A study of the uncertainty in predictions for Z + jets final states from different matrix element + Monte Carlo calculations is given in Ref. [9].

events are generated with a filter requiring two electrons/muons with $p_T > 5$ GeV and $|\eta| < 2.8$. For $Z \to \tau^+ \tau^-$ and $Z \to e^+ e^-$, the dilepton mass is required to be larger than 60 GeV. A large QCD dijet sample (3.3M events) with a minimum hard-scattering transverse momentum of 17 GeV is also used.

2.2 Corrections from Parton to Hadron Level

Cross-section measurements in data and LO/NLO predictions are to be compared at the hadron level (particle level). Hence, the data have to be unfolded with respect to the detector response. For comparisons of data to NLO parton level predictions from MCFM, either the data need to be corrected to the parton level or the theory corrected to the hadron level. We discuss the latter correction below for the specific case of $Z +$ jets (but which can also be applied without great error to the case of W + jets). The MCFM predictions have to be corrected with respect to the non-perturbative effects of fragmentation and underlying event (UE). The fragmentation and underlying event corrections are extracted using PYTHIA Monte Carlo samples by comparing the hadron level results, with the current ATLAS underlying event tune, to corresponding results in samples in which fragmentation and multiple-parton-interactions have been switched off. The corrections are determined by dividing the hadron-level distribution of the observables from standard PYTHIA by the respective distributions from PYTHIA with the non-perturbative effects switched off. To the extent to which the two partons that can comprise a jet in MCFM mimic the effects of the parton shower in PYTHIA, the corrections derived from the procedure above can be applied to the MCFM output [3]. The hadronization corrections depend in principle on both the type of jet algorithm and the corresponding size parameter. For jets with radius 0.4, the non-perturbative effects are observed to be negligible for $p_T > 40$ GeV/c. A residual correction at the percent level is applied to the MCFM cross sections.

3 Particle ID and Trigger

We adopt as much as possible definitions and cuts in common with the other notes, and in particular with the inclusive W/Z note [1], with comparisons to alternate definitions/cuts where relevant. The reconstruction algorithms in this note are not necessarily optimal for the running conditions in the first two years, but provide a reasonable baseline. We expect further optimization as data become available.

3.1 Electrons

The electron candidates are required to have $p_T > 25$ GeV, and to lie in the range $|\eta| < 2.4$, excluding the barrel-to-endcap calorimeter crack region $(1.37 < |\eta| < 1.52)$. The electrons are required to fulfill the medium electron-ID signature [2] [11], which consists of requirements on the calorimeter shower-shape and the matched track. The Z selection requires two electron candidates with an invariant mass of $81 < m_{ee} < 101$ GeV and $\Delta R > 0.2$ between the electrons.[3]

---

[2] General criteria corresponding to tight and loose electron ID are also available, with tight(loose) resulting in a lower (higher) efficiency, and a smaller (larger) background.

[3] No calorimeter isolation cuts are applied for these analyses, due to simulation problems, but will be in the actual data analyses. There is an implicit isolation cut, however, present in the trigger [12].

3.2 Muons

A muon candidate requires the combined reconstruction of an inner detector track and a track in the muon spectrometer [13]. Muons are required to have $p_T > 15$ GeV and $|\eta| < 2.4$, with the range $1.2 < |\eta| < 1.3$ being excluded. Isolation is applied by requiring the energy deposition in the calorimeter to be less than 15 GeV in a cone of $\Delta R = 0.2$ around the extrapolation of the muon track. Two muon candidates are selected with an invariant mass of $81 < m_{\mu\mu} < 101$ GeV.

3.3 Jets

For the analyses in this note, we use jets clustered with the standard ATLAS Seeded Cone algorithm with a radius of $R = 0.4$ (appropriate for the complex final states expected for the multi-jet environments explored in this note), built from calorimeter towers ($Z \to e^+e^-$ analysis) and topological clusters [4] ($Z \to \mu^+\mu^-$ analysis), and calibrated to the hadron level. A detailed comparison with other jet algorithms, including the k_T algorithm, is beyond the scope of this note. The lepton and jet candidates must be separated by $\Delta R_{lj} > 0.4$. It is required that the jet transverse momentum be $p_T > 20$ GeV in the range $|\eta| < 3.0$. The cross-section measurements themselves are prepared only for jets with $p_T > 40$ GeV.

3.4 Trigger Paths

The trigger selection used here is the same as that used in the inclusive analyses [1]. In the electron channel, $Z \to e^+e^-$ + jets events are required to pass the isolated dielectron trigger or the isolated single-electron trigger. In the muon channel, $Z \to \mu^+\mu^-$ + jets events are required to pass the isolated dimuon trigger. The trigger efficiencies at the first, second and event filter levels are evaluated as a function of the jet multiplicity. The trigger efficiency is also studied as a function of the overall hadronic activity, the p_T of the leading jet and the Z transverse momentum. For this purpose, the generated Monte Carlo information and the data driven tag-and-probe method are compared. Good agreement between the two methods is found. The overall trigger efficiency, with respect to that for the off-line cuts, for the inclusive analysis is compared to that obtained here. It is found that the trigger efficiency for the Z+jets analysis is, in general, $1.5 - 2\%$ lower than that of the inclusive sample.

4 Measurement of Z + Jets Cross-Sections

4.1 Introduction

This Section discusses the study of the inclusive $Z(\to e^+e^-, \mu^+\mu^-)$ + jets cross-sections as a function of the jet transverse momentum and jet multiplicity. The pseudo-data is compared with LO and NLO perturbative QCD predictions. These analyses will be used, in addition, to validate the event generators which are used to predict the $Z(W)$+jets backgrounds for searches in ATLAS.

In order to prepare the measurement, we use fully-simulated signal and background Monte Carlo events as pseudo-data, with which we perform all steps of the analysis. In some cases, we also compare the predictions of fully simulated signal Monte Carlo sets from different event generators. The goal of the analysis simulation is to validate the lepton and jet reconstruction in high jet multiplicity events, develop the necessary analysis techniques (unfolding, background subtraction) and evaluate the statistical and systematic limitations in terms of probing the QCD predictions. Two separate,

---

[4] Topological clusters are groups of calorimeter towers calibrated back to approximately the hadron level.

Process	$Z \to e^+e^- + \geq 1$jet xsec	$Z \to e^+e^- + \geq 1$jet fraction	$Z \to e^+e^- + \geq 2$jets xsec	$Z \to e^+e^- + \geq 2$jets fraction	$Z \to e^+e^- + \geq 3$jets xsec	$Z \to e^+e^- + \geq 3$jets fraction
$Z \to e^+e^-$	23520 ± 145	91.9 ± 0.8	4894 ± 45	87.9 ± 1.3	900 ± 15	80.0 ± 2.4
QCD jets	1545 ± 89	6.0 ± 0.4	336 ± 42	6.0 ± 0.8	78 ± 20	6.9 ± 1.8
$t\bar{t}$	496 ± 28	1.9 ± 0.1	333 ± 23	6.0 ± 0.4	146 ± 15	13.0 ± 1.4
$Z \to \tau^+\tau^-$	3.2 ± 1.2	0.01 ± 0.005	(0.67 ± 0.25)	(0.01 ± 0.005)	(0.1 ± 0.05)	(0.01 ± 0.005)
$W \to e\nu$	(28 ± 13)	(0.1 ± 0.05)	(5.9 ± 2.6)	(0.1 ± 0.05)	(1.1 ± 0.5)	(0.1 ± 0.05)

Table 1: The accepted cross-sections (in fb) and the corresponding surviving fractions (in %) from signal and background in the $Z \to e^+e^- +$ jets analysis, after applying the cuts outlined in Section 3. The jet transverse momenta are required to be greater than 40 GeV. The numbers in brackets are extrapolated from results obtained for a lower jet multiplicity.

but related, studies are performed on the feasibility of the $Z \to e^+e^-$ and the $Z \to \mu^+\mu^-$ channels (Sections 4.2 and 4.3).

4.2 $Z \to e^+e^-$ + Jets

4.2.1 Signal and Background Distributions

The presence of additional jets in the event has an impact on the kinematics of both the leptons and jets. The distributions of electron p_T, jet p_T, ΔR between electrons and the minimum ΔR between each electron and the jets (for different jet multiplicities) are studied using fully-simulated $Z \to e^+e^-$ samples. As expected, the electrons are more boosted (larger p_T and lower ΔR between electrons) in events with jets, and the distance between electrons and jets becomes smaller in high-multiplicity events. The average jet p_T increases with the number of jets. Due to the OR of the single electron and dielectron trigger channels used in this analysis, any efficiency loss of the isolated electron triggers for large jet multiplicities has only a negligible impact. The total Z reconstruction efficiency (offline+trigger) is stable with respect to both the jet multiplicity and the transverse momentum of the leading jet.

4.2.2 Background Estimation

The most important backgrounds to the $Z \to e^+e^- +$ jets signal are processes with real electrons ($t\bar{t}$, $W \to e\nu$, $Z \to \tau^+\tau^-$) and QCD jet production. Statistics of the QCD background sample are increased by applying a very loose electron selection and then reweighting the events with the additional rejection factor for the final electron ID. The combined distribution of the invariant mass for signal and background events is shown in Fig. 1(a) for the $Z + 1$ jet inclusive cross section. Table 1 gives an overview of the accepted cross-section expected from Monte Carlo from signal and backgrounds for several jet multiplicities. With increasing jet multiplicity, $t\bar{t}$ replaces QCD as the dominant background source. The errors displayed in the Table are of statistical nature only. Systematic errors stemming from the QCD reweighting, and from comparing the results of different generators, are not included in this Table. Eventually, the QCD background will be determined with data driven methods. The simulation of the $t\bar{t}$ background will also have to be validated separately with data. Figures 1(b)-(d) show the distribution of signal and backgrounds for the observables (jet multiplicity and $p_{T\,\text{jet}}$).
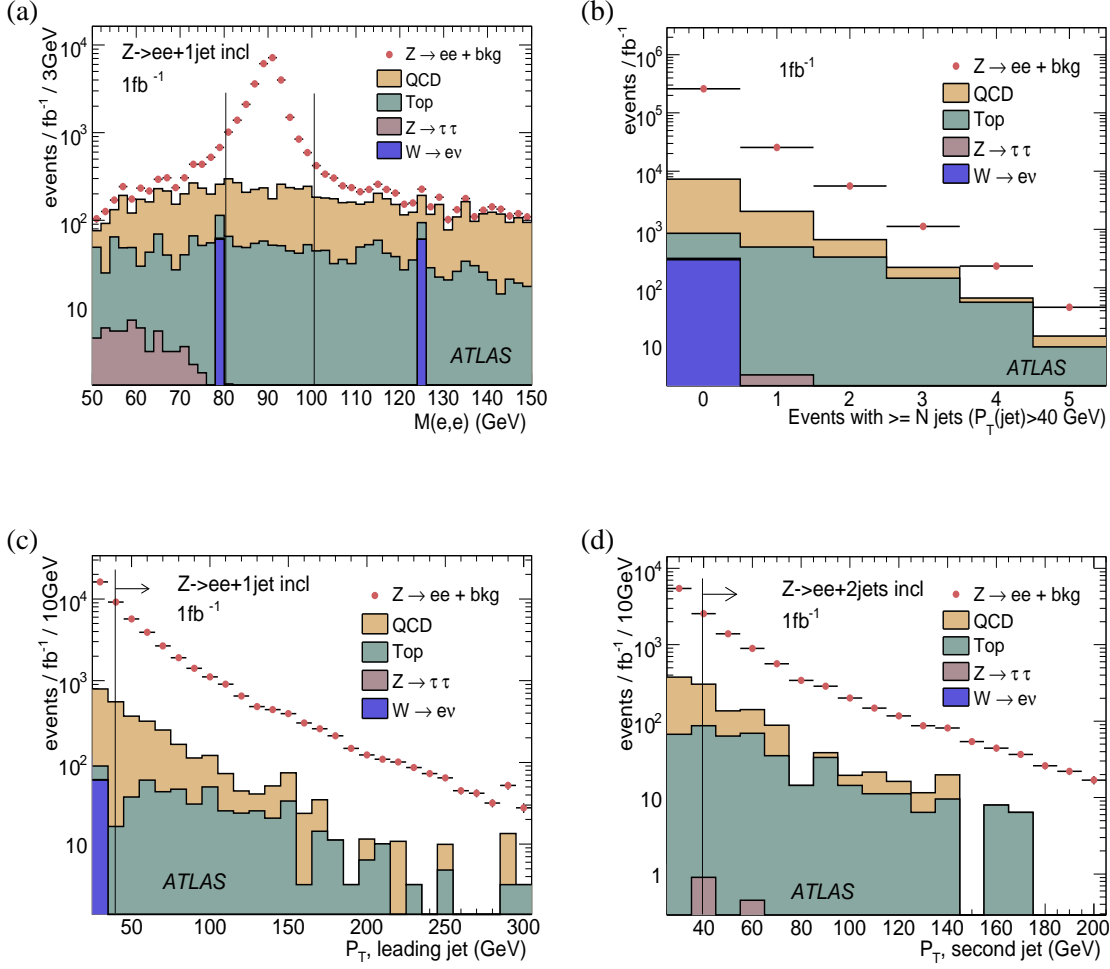
Figure 1: The distribution of the dielectron mass for signal and background for (a) $Z \to e^+ e^- + \geq 1$jet,; the number of events with $\geq$ N jets ($p_T > 40$ GeV) (b) and of the p_T of the leading (c) and the next-to-leading (d) jet for $\int L\,dt = 1\,\text{fb}^{-1}$.

4.2.3 Unfolding of Detector Effects

The reconstructed data have to be unfolded from the detector level to the hadron level, correcting for efficiency, resolution and non-linearities in electron and jet reconstruction. In this note, the individual unfolding corrections are assumed to factorize in leading approximation, and the individual contributions are investigated separately. For the data analysis, an approach will be used consisting of unfolding the combined impact of jet reconstruction efficiency and jet resolution in a bin-by-bin unfolding procedure. Since the dominant correction (electron efficiency) is independent of the jet transverse momentum, the difference between the two approaches should be minimal. The corrections are derived with fully-simulated Monte Carlo. The simulation of the jet calibration and resolution will have to be validated with real data.

The event weight is corrected for the electron reconstruction efficiency. Since this is the dominant correction and since it varies strongly with both pseudorapidity and with the transverse momentum

of the electron, the correction is derived as a function of the generated $|\eta|$ in four bins of generated p_T. The event weight is also corrected for the global efficiency for the electron trigger with respect to the offline selection, determined as: $\mathrm{eff_{trig}} = (99.63 \pm 0.11)\%$. The errors on deriving this efficiency, stemming from the limited Monte Carlo statistics, are taken into account as systematic errors for the unfolding procedure. The jet observables are corrected for shifts in the measured jet energy scale (mainly non-linearities at low p_T), the jet energy scale resolution and the jet reconstruction efficiency. All corrections are derived for ten bins in p_T with a comparable number of events in each bin in order to avoid large statistical fluctuations. The jet p_T scale and resolution are determined using a matching window of the ΔR distance between the Monte Carlo and reconstructed jets, $\Delta \mathrm{R}(MC - reco\,jet) < 0.2$ and the ratio of the reconstructed to the generated Monte Carlo jet p_T, $0.5 < p_T(reco)/p_T(MC) < 1.5$. The jet reconstruction efficiency is determined as the fraction of the Monte Carlo jets which are matched to reconstructed jets applying the same requirements. As expected, the largest bias is observed for low values of $p_{T\,\mathrm{jet}}$. The impact of the resolution is derived by comparing the p_T distribution of the Monte Carlo jets before and after a gaussian smearing with the resolution as determined above. A global average correction for the two effects of 0.984 ± 0.005 is determined for jets with $p_T > 40$ GeV.

The reconstructed jet p_T is corrected with the jet energy scale corrections, and the event is weighted for each required jet with the correction for efficiency-loss in reconstruction, and the over-population due to the jet p_T resolution. The unfolding corrections are validated by comparing the distributions of the Monte Carlo jet variables with the corresponding ones for corrected reconstructed jets. Within the statistical and systematic errors, the p_T distributions of the Monte Carlo jets and corrected reconstructed jets are in agreement, thus validating the unfolding corrections.

4.2.4 Background Subtraction

The $Z \to \tau^+\tau^-$, $t\bar{t}$ and $W \to e\nu$ backgrounds are subtracted using the Monte Carlo estimates, as can also be done for the collision data. Special care has to be exercised in validating the differential cross section for the $t\bar{t}$ background, since it is the dominant background source for large jet multiplicities. Data-driven approaches to extract the $t\bar{t}$ background are being developed. The QCD background is subtracted by weighting all events with a global factor, calculated as 1 - QCD-fraction (as in Tab. 1). For the final simulation of the measurement, signal and background samples are combined and unfolded to the hadron level, as described above.

4.3 $Z \to \mu^+\mu^-$ + Jets

The impact of a high jet multiplicity environment on the lepton reconstruction efficiency is also investigated for the case of the muon channel, and the measurement of $Z +$ jets final states discussed using similar techniques as discussed for the electron channel in Section 4.2.1. Muon reconstruction efficiencies for different isolation requirements are also investigated.

4.3.1 Background Estimation

The important backgrounds for the $Z \to \mu^+\mu^- +$ jets analysis are processes of similar topologies ($t\bar{t}$, $W \to \mu\nu$, $Z \to \tau^+\tau^-$) with real muons, and QCD multi-jet production. For $t\bar{t}$, $W \to \mu\nu$ and $Z \to \tau^+\tau^-$ PYTHIA and ALPGEN Monte Carlo samples are used. It can be assumed that the dominating QCD dijet contribution of highly energetic muons are from decays of $b\bar{b}$ mesons. Monte Carlo samples generated with PYTHIA $b\bar{b}(\to \mu^+\mu^-)$ are thus used to increase the muon background statistics. Within the Z mass window, the dominant background is from top pair production.

4.3.2 Signal and Background Distributions

Muons from $Z \to \mu^+\mu^-$ are highly energetic and isolated. For low jet multiplicities, $b\bar{b}$ production, with semileptonic b decays into muons, is the dominant background source. It can be efficiently suppressed by an isolation cut which requires the energy deposited in the calorimeter in a cone of $\Delta R = 0.2$ around the muon to be less than 15 GeV. The cut is optimized such that it maximizes the background suppression without introducing a bias in the reconstruction efficiency for high jet multiplicities. Table 2 shows the accepted cross-sections and the surviving fraction of signal and background for different jet multiplicities using PYTHIA and ALPGEN for the background determinations. For $Z \to \mu^+\mu^- + \geq 3\text{jets}$ events, the $t\bar{t}$ background fraction increases to 13% (PYTHIA) and 20% (ALPGEN). The lower rate predicted by PYTHIA for $t\bar{t} \to ll+3$ jets is due to the third jet being produced by the parton shower instead of the hard matrix element used in ALPGEN.

Figure 2 shows the inclusive jet multiplicity for the signal and backgrounds simulated with the PYTHIA (a) and ALPGEN (b) Monte Carlo data samples. Figure 2(c)-(f) shows the distributions for signal and background for the leading and next-to-leading jets simulated with PYTHIA (c),(e) and ALPGEN (d),(f). In general, the top background is larger from ALPGEN than from PYTHIA, with the difference being a reasonable estimate of the uncertainty.

Process	$Z \to \mu^+\mu^- + \geq 1\text{jet}$ xsec	$Z \to \mu^+\mu^- + \geq 1\text{jet}$ fraction	$Z \to \mu^+\mu^- + \geq 2\text{jets}$ xsec	$Z \to \mu^+\mu^- + \geq 2\text{jets}$ fraction	$Z \to \mu^+\mu^- + \geq 3\text{jets}$ xsec	$Z \to \mu^+\mu^- + \geq 3\text{jets}$ fraction
PYTHIA						
$Z \to \mu^+\mu^-$	72819±784	96.9±1.0	11660±314	89.4±2.4	1974±129	87.7±2.5
$W \to \mu\nu$	0±183	0.0±0.2	0±31	0.0±0.2	0±5	0.0±0.2
QCD($b\bar{b}$)	1225±541	1.6±0.7	599±304	4.6±2.3	0±113	0.0±5.0
$t\bar{t}$	1141±110	1.5±0.1	789±92	6.0±0.7	277±54	12.3±2.4
total background	2366±582	3.1±0.7	1388±319	10.6±2.4	277±125	12.3±5.5
ALPGEN						
$Z \to \mu^+\mu^-$	59408±644	96.1±1.0	12568±276	88.7±1.9	2446±100	79.6±3.3
$W \to \mu\nu$	22±20	0.0±0.0	0±17	0.0±0.1	0.0±0.4	0.0±0.1
QCD($b\bar{b}$)	1225±541	1.6±0.7	599±304	4.6±2.3	0±113	0.0±5.0
$t\bar{t}$	1163±159	1.9±0.3	1008±150	7.1±1.0	626±119	20.4±3.9
total background	2310±564	3.9±0.9	1607±339	11.3±2.3	626±164	20.4±5.4

Table 2: The accepted cross-sections (in fb) and the corresponding surviving fractions (in %) from signal and background in the $Z \to \mu^+\mu^- +$ jets selection for different jet multiplicities, after applying the cuts outlined in Section 3. The transverse momentum of jets is required to be greater than 40 GeV.

4.4 Comparison of Event Generators and MCFM at the Hadron Level

We consider the comparison of theory and measurement for theoretically well-defined quantities: the inclusive cross-section for $Z \to \ell\ell + \geq 1\text{jet}$, $Z \to \ell\ell + \geq 2\text{jets}$ and $Z \to \ell\ell + \geq 3\text{jets}$ and the differential cross-sections with respect to the p_T of the leading and the next-to-leading jets. The MCFM predictions are corrected for the residual energy loss due to non-perturbative effects for jets with $p_T > 40$ GeV, determined from the current PYTHIA tune of underlying event and fragmentation as 0.98 ± 0.01 for $Z \to \ell\ell + \geq 1\text{jet}$, 0.98 ± 0.02 for $Z \to \ell\ell + \geq 2\text{jets}$ and 0.95 ± 0.06 for $Z \to \ell\ell + \geq 3\text{jets}$. PDF uncertainties on the MCFM predictions are calculated using the complete set of error PDFs from the CTEQ6.1 PDF set. The inclusive PYTHIA and ALPGEN $Z \to \ell^+\ell^-$ samples are normalized to the NLO inclusive MCFM $Z \to \ell^+\ell^-$ cross-section at the generator level.
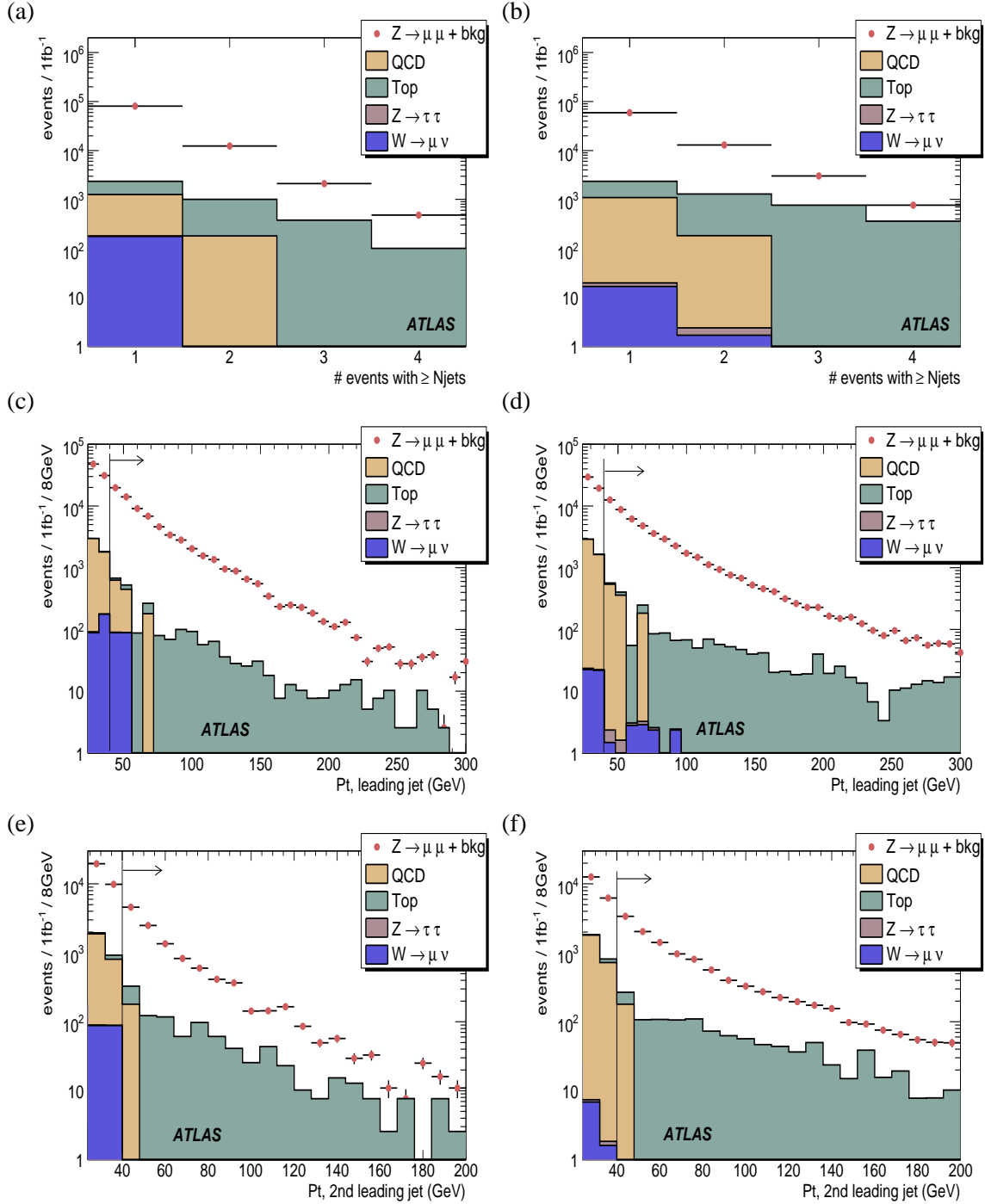
Figure 2: Distributions of $Z \rightarrow \mu^{+}\mu^{-}$ signal and background jet multiplicities, with backgrounds determined by PYTHIA (a) and ALPGEN (b). The jets in this plot are required to have a transverse momentum greater than 40 GeV. The leading jet p_T and 2nd leading jet p_T distributions for signal and background using PYTHIA (c),(e) and ALPGEN (d),(f) data samples to determine the backgrounds. In order to provide higher statistics for the background determination, the background events in an invariant mass window of $51 - 131$ GeV, are scaled down for an invariant mass window of $81 - 101$ GeV.

Figures 3(a)-(c) show the comparison [5] of the distribution of the observables (jet multiplicities and the p_T of the leading and next-to leading jets) at the hadron level for ALPGEN and PYTHIA Monte Carlo with LO and NLO MCFM calculations. The fully simulated ALPGEN and PYTHIA samples are unfolded to the hadron level as described in Section 4.2.3. The error bars are calculated only from intrinsic Monte Carlo quantities as the quadratic sum of statistical errors from the Monte Carlo sample size and the systematic errors from the unfolding corrections derived from Monte Carlo. The shape of the jet p_T distribution predicted by ALPGEN agrees well with the shape predicted by MCFM. Due to the tuning of the leading soft radiation in the parton shower, PYTHIA predicts a larger inclusive cross-section for $Z \to e^+e^- + \geq 1$jet but a clearly softer p_T spectrum.

As a further step towards real ATLAS data, the systematic errors are adjusted to the values expected from the collision data and propagated to the measured cross-section. Figure 3(d) shows the relative systematic uncertainty on the cross-section (normalized to 1) expected for different uncertainties on the jet energy scale for the production of a Z with 1-4 jets ($p_T > 40$ GeV). Since the difference between the LO and NLO cross-section predictions (for the given renormalization/factorization scale choices) are on the order of 30%, with a 3% uncertainty on the jet energy scale, we are still able to differentiate between LO and NLO predictions, whereas with an error of 10% on the jet energy scale this is not possible. For comparison, the statistical error expected for the 4 jet bin is of the order of 5% (correspondingly less for the lower jet multiplicities) and the PDF uncertainty for all jets bins is less than 5%. The uncertainty on the jet energy resolution and its impact on the unfolding procedure is an additional source of systematic error on the cross-section measurement. They are investigated for jet resolutions up to two times the ones currently expected. An uncertainty of 50% on the jet resolution propagates to an error of 2-4% on the $Z \to e^+e^- + \geq 1$jet cross-section measurement. A wrong assumption of the jet p_T distribution in calculating the unfolding corrections from the jet energy resolution can also lead to a systematic shift in the cross-section measurement. A comparison between the unfolding corrections derived from PYTHIA and from ALPGEN yields a systematic uncertainty of up to 1.5 %.

5   Conclusions

Final states containing Z + jets will serve as one of the standard model benchmarks for physics analyses at the LHC. These states form the signal channels (as well as the backgrounds) for known standard model processes such as $t\bar{t}$ production, as well as beyond standard model signals such as supersymmetry. In the first inverse femtobarn, ATLAS will observe more than 300 Z + four or more jets (with $p_T > 40$ GeV/c) in both the dielectron and dimuon channels. The events will be triggered by the presence of the energetic decay lepton from the Z). The presence of additional jets in the events will tend to boost the Z, and thus the decay leptons, to higher transverse momentum, leading to a larger acceptance. The presence of the jets will also tend to negatively affect the lepton analysis cuts, such as on isolation. The two effects roughly cancel out, resulting in total efficiencies in general a few percent lower than for the inclusive analyses.

$Z \to e^+e^-, \mu^+\mu^-$ + jets events suffer from backgrounds involving real electrons and muons (from $t\bar{t}, Z \to \tau^+\tau^-$ and $W \to e\nu(\mu\nu)$ and from backgrounds involving fake electrons and muons (QCD jet production). The former can be reliably estimated from current Monte Carlo predictions, although in situ verification with data will be needed, while the latter, dealing with rare fluctuations of large cross-

---

[5] For reasons of space, we restrict ourselves to comparisons to the electron channel. Equivalent results have been obtained for the muon channel, using a different jet reconstruction technique (topological clusters) and a different unfolding technique.
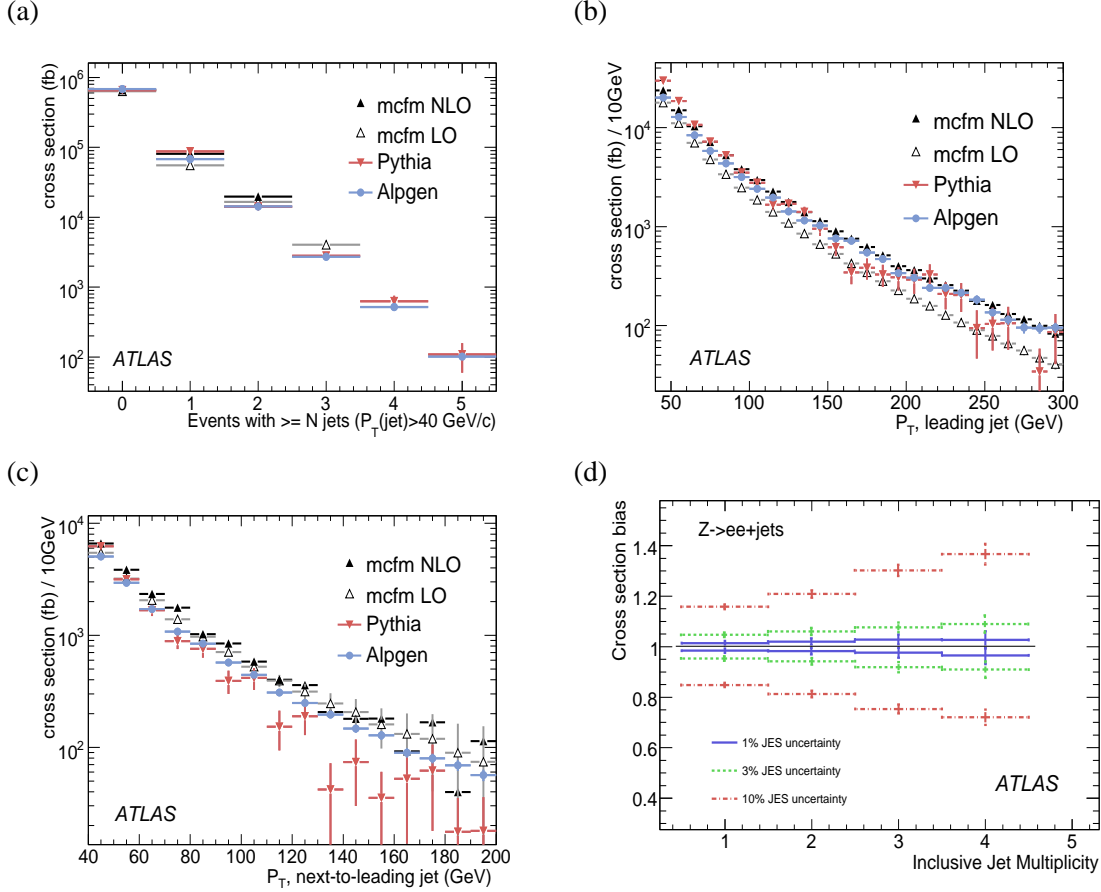
Figure 3: The inclusive jet cross-section for the $Z \to e^+e^-$ analysis as a function of jet multiplicity is shown in (a); the p_T of the leading jet (b) and of the next-to-leading jet (c) are shown for the unfolded PYTHIA and ALPGEN Monte Carlo predictions and for MCFM for an $\int L\,dt = 1\,\text{fb}^{-1}$. In (d), the relative systematic uncertainties on the cross-section (normalized to 1) are shown for different uncertainties on the jet energy scale. All jets are required to have a transverse momentum greater than 40 GeV.

section processes can only be crudely estimated from current Monte Carlo simulation. An estimate for the QCD background is made from the existing Monte Carlo event samples, and a scheme to determine the background from the real data is outlined. In this note, lacking data, we have compared background predictions from PYTHIA and ALPGEN(+HERWIG). The backgrounds increase with jet multiplicity, with $t\bar{t}$ being the largest background for high jet multiplicities, and with QCD jet production dominating the background for low jet multiplicities. The backgrounds for $W \to e\nu, \mu\nu$ + jets events result from similar sources as for the Z case (with the $Z \to e^+e^-, \mu^+\mu^-$ background replacing the $W \to e\nu(\mu\nu)$ one). With the cuts used in the analyses presented in this note, the W and Z + jets signal is substantially larger than the sum of the backgrounds, while maintaining reasonable efficiency. Experience with actual data will help to improve this discrimination further.

In this note, we have considered cross-section measurements for theoretically well-defined quantities. The cross-sections for W/Z + jets in ATLAS will be quoted at the hadron level, corrected for all detector measurement effects. An unfolding technique, from the detector to the hadron level, which

can be used with actual data as well as with fully simulated Monte Carlo events, is developed for this note. The corrections from parton to hadron level, necessary for comparisons to parton level predictions, have also been determined. The two main non-perturbative effects, due to the underlying event and to the jet fragmentation, result in corrections in opposite directions that partially cancel, and in any case are expected to be at the percent level for transverse momentum larger than 40 GeV.

The dominant systematic error in the cross-section measurements will be due to the uncertainty in the jet energy scale. We have considered the impact of jet energy scale uncertainties of 10%, as expected in the very early running, of 3%, as might be achieved after 2 years of running, and of 1%, an optimistic goal after the detector is well-understood.

References

[1] ATLAS Collaboration, W/Z inclusive cross-section, this volume

[2] ATLAS Collaboration, ATLAS reference cross-section note, this volume

[3] J. M. Campbell, J. W. Huston and W. J. Stirling, Rept. Prog. Phys. **70**, 89 (2007) [arXiv:hep-ph/0611148].

[4] J. Campbell, R.K. Ellis, $http://mcfm.fnal.gov/$;J. Campbell, R.K. Ellis, Phys. Rev. **D65** 113007 (2002).

[5] D. Stump, J. Huston, J. Pumplin, W. K. Tung, H. L. Lai, S. Kuhlmann and J. F. Owens, JHEP **0310**, 046 (2003) [arXiv:hep-ph/0303013].

[6] M.L. Mangano, M. Moretti, F. Piccinini, R. Pittau and A. Polosa, JHEP **0307** (2003) 001.

[7] G. Corcella *et al.*, JHEP **0101**, 010 (2001) [arXiv:hep-ph/0011363].

[8] J. Pumplin, D. R. Stump, J. Huston, H. L. Lai, P. Nadolsky and W. K. Tung, JHEP **0207**, 012 (2002) [arXiv:hep-ph/0201195].

[9] J. Alwall *et al.*, Eur. Phys. J. C **53**, 473 (2008) [arXiv:0706.2569 [hep-ph]].

[10] T. Sjostrand *et al.,* Comp. Phys. Commun.**135** (2001) 238.

[11] ATLAS Collaboration, Electron ID, this volume

[12] ATLAS Collaboration, L1 Calorimeter trigger performance, this volume

[13] ATLAS Collaboration, Muon reconstruction and ID performance, this volume